Applied Chemical Engineering (2025) Volume 9 Issue 2 ISSN: 2578-2010 (O)
doi: 10.59429/ace.v9i2.5888

RESEARCH ARTICLE

Thermoelectric properties of naphthalene bridge tetracyanoquinodimethane based molecular Junctions

Asrra Modhir Habeeb[1], Hussein Neama Najeeb[2*], Qussay Mohammed Salman[3]

[123] *Babylon University, College of Science for Women, Iraq*

***Corresponding author:** Hussein Neama Najeeb, husseinnajeeb98@gmail.com

ABSTRACT

This determined the electrical characteristics of the six-naphthalene bridge tetracyanoquinodimethane dye that were suggested. The characteristics were determined by plotting energy and temperature against one another. The SIESTA-trunk-426 program was used for the relaxation of the dyes under study by employing the Generalized Gradient Approximation/Double Zeta Density Functional Theory (GGA/DZ-DFT). The Gollum program was employed for The SIESTA-trunk-426 algorithm was used to relax the dyes under examination using the Generalized Gradient Approximation/Double Zeta Density Functional Theory (GGA/DZ-DFT). Calculating the electrical characteristics of the dyes under study. Initially, each dye was inserted between two gold electrodes, and the dye, along with the confined layers of the electrodes, were allowed to react a second time to form the relaxed structures. Electrical conductivity, conductance, thermal conductivity, and the Seebeck coefficient were examined.

Keywords: DFT; Conductance; Seebeck Coefficient; Naphthalene.

ARTICLE INFO

Received: 15 January 2026
Accepted: 01 April 2026
Available online: 17 April 2026

1. Introduction

Tetracyanoquinodimethane (TCNQ)-based molecules are extensively utilized for their electrical and magnetic properties [1-4]. The electron-accepting capabilities of TCNQ derivatives have been investigated by augmenting their π-system [5-9]. This π-system extension, derived from cyclic voltammetry (CV) data, which reveals greater negative reduction potentials relative to TCNQ, suggests that TCNQ derivatives are inferior electron acceptors compared to TCNQ [6]. However, π-extended TCNQ derivatives, characterized by elevated electron affinities, have been documented to be novel n-type organic semiconductors [10-13]. Conversely, less symmetrical TCNQ derivatives exhibit superior molecular packing, resulting in enhanced electron-accepting capability in the solid state. A required characteristic of n-type semiconductors is elevated electron affinity. Two more critical factors to consider are the molecule conformation, which influences solid-state packing, and the capacity to receive and transport electrons. Currently, numerous organic p-type semiconductors have been developed for practical applications in organic field effect transistors (OFETs); still, only a limited amount of high-performance solution-processed n-type organic thin film transistors have been documented [14-17]. The disparity in development enables the investigation of prospects for n-type semiconductors extremely advantageous. In the development of novel n-type semiconductor molecules, we concentrate on less symmetrical TCNQ derivatives, as TCNQ imparts significant

electron affinity to the system. Additional significant aspects that may influence charge carrier mobility are also taken into consideration. The factors encompass the increase in the number of rings, the integration of nitrogen atoms with high electron affinity, and the reduced energies of the highest occupied molecular orbital (HOMO) and lowest unoccupied molecular orbital (LUMO) of the molecule.

2. Computational Methods

The electronic structures of all dyes were initially calculated using a double-ζ polarized zeta (DPZ) basis set. To elucidate the experimentally observed trends and enhance understanding of the transport properties of these molecular junctions, calculations were conducted utilizing a combination of density functional theory (DFT) through the SIESTA code and the non-equilibrium Green's function (NEGF) formalism. The DFT-Landauer method employed in the modeling presupposes that electron transport through the molecule transpires on a rate that renders inelastic scattering negligible—an assumption deemed valid for molecules extending up to several nanometers in length. In the transport computations, each molecule was linked to opposing gold electrodes configured as 35-atom pyramids aligned along the (111) crystal direction. The SIESTA code, which is based on density-functional theory and employs the generalized gradient approximation (GGA) [19], was subsequently used for geometric optimization. In order to assess binding energies and ideal geometries, DFT was used to determine the ground-state energy of various molecular junctions.

3. Results and Discussion

Figure 1 displays the dyes' relaxed structures. Each dye, R1, R2, R3, R4, R5, and R6, was attached at the terminal ends to gold electrodes via sulfur atoms as anchor groups after the determination of the suitable distance.

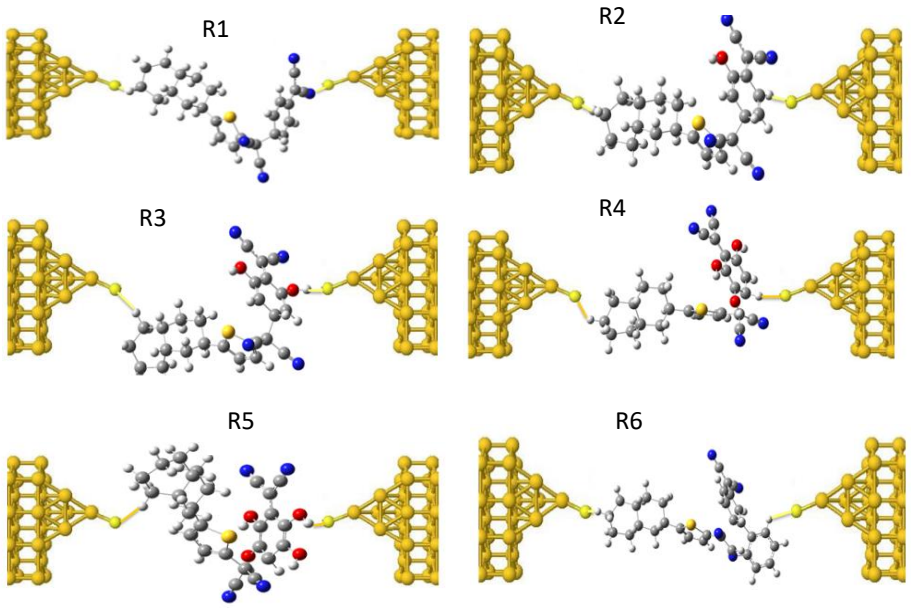

Figure 1. The relax structures of the dyes.

The dyes' electrical conductivity vs Fermi energy is shown in Figure 2. Dye electrical conductivity values were altered at room temperature in the energy range of -1 to 1 eV in Siemens (S). Dye numbers R1, R2, R3, R4, R5, and R6 have electrical conductivities of $1.5x10^{-9}$, $2.5x10^{-9}$, $8.8x10^{-9}$, $3.7x10^{-9}$, $6.6x10^{-9}$, and $1.2x10^{-8}$ S, respectively, up to the Fermi level, where E-EF= 0. This finding highlights the significance of the function groups located at the terminals of the dye's ligands. The electrical conductivity value of dye R6 is the highest.

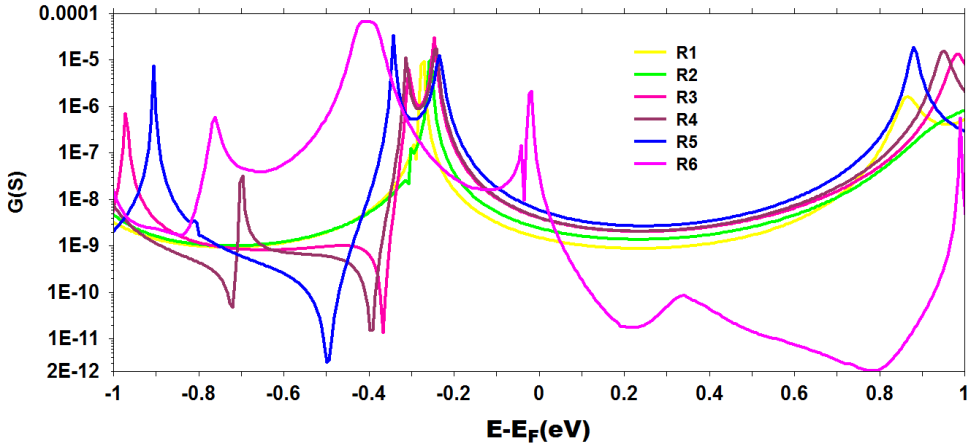

Figure 2. Electrical conductivity of the dyes

As seen in Figure 3, the dyes' conductance G/G_o is a function of energy. Room temperature conductance values varied in the following order, as shown in the figure: This order of importance is as follows: R6 > R5 > R4 > R3 > R2 > R1.

The outcome reflects how well the dyes were coordinated. The highest value of G/G_o, which is 0.00305, is found in dye R6. The lowest value of G/G_o for dye R1 is 2.311 $x10^{-5}$. The G/G_o values for dyes R2, R3, R4, and R5 are 0.000108, 7.347 x 10^{-5}, 7.563 x 10^{-5}, and 3.857 x 10^{-5}, respectively. The minimum and maximum values of G/G_o for all dyes are correspond to positive values of energy, except for dye R6.

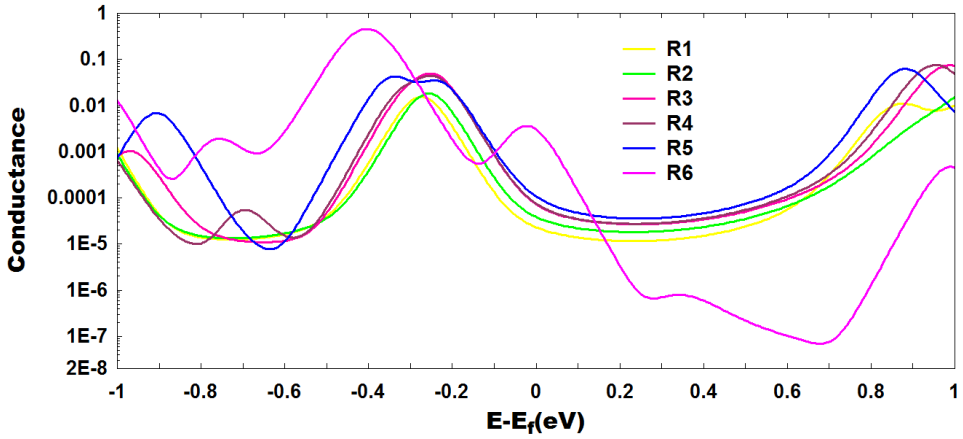

Figure 3. G/G_o of the dyes

Conversely, Figure 4 shows the G/G_o behavior of the investigated dyes over a temperature range of 0–400 K. After reaching a small increase at T= 50 K, the conductance continued to rise until it reached its stable value at T = 180 K. Among the dyes tested, R2's G/G_o value is the most consistent across the temperature range of 180–400 K. At T=50 K, the G/G_o value of dye R4 is 0.1518227, which is high, and it drops to 0.0468503 after cooling. The findings displayed in Figure 4 indicate that the tunneling conductance of single-molecule junctions is temperature dependent and can exhibit small variations between 50 K and 400 K. These calculations cannot be explained by changes in the Fermi distribution due to temperature smearing. My theory is that tunneling transport across single molecule-metal junctions can be impacted by a small temperature-dependent change in the interface structure between the metal and the molecule. While the gold relaxes into a smoother shape at high temperatures, the electrodes retain their extremely corrugated and sharp characteristics at low temperatures. This explains the observed conductance shift with temperature by influencing the alignment of the molecular orbitals relative to the metal Fermi level.

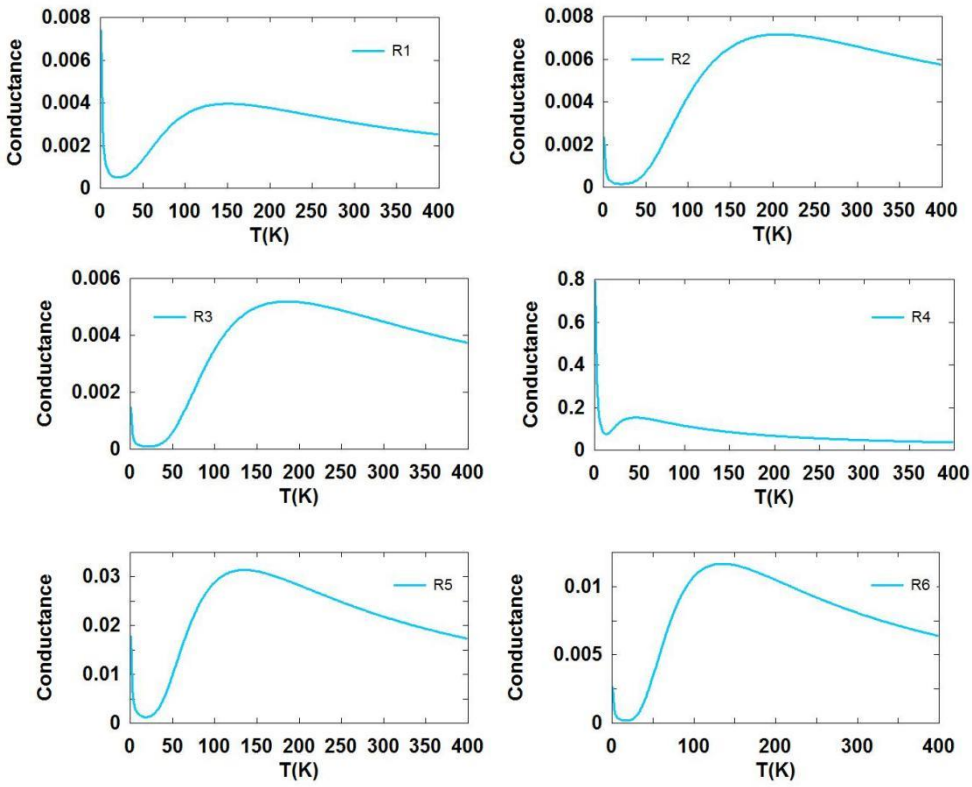

Figure 4. Conductance as a function of temperature for the dyes

The thermal conductivity of the dyes, measured in W/m.K, is shown in Figure 5 for the temperature range of 0 to 400 K. The investigated dyes exhibited, on the whole, modest thermal conductivity values. At almost freezing temperatures, the conductance of R1, R2, and R3 is low. It grows as the temperature rises up to a maximum, after which it starts to drop again. Conductance increases with thermal energy up to a certain point, and then it drops due to factors like scattering; this behavior suggests that these materials might be semiconductors. Dyes R4, R5, and R6 behave similarly, with conductance starting low, increasing with temperature, and then decreasing at higher temperatures. The difference could be in the peak conductance values or the temperature range in which these changes occur. The behavior displayed reflects the typical temperature dependency of conductance in semiconducting materials. At low temperatures, there are very few electrons accessible for conduction. As temperature rises, more electrons are liberated as a result of thermal energy, resulting in increased conductance. Electron scattering and other processes begin to have a negative impact on conductivity at extremely high temperatures.

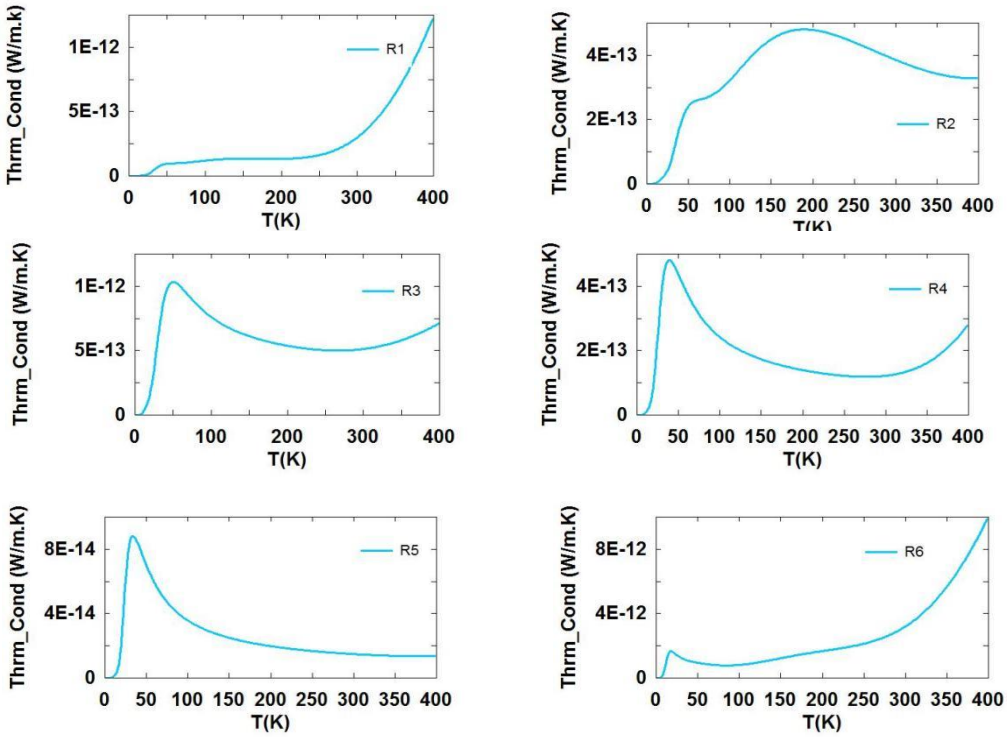

Figure 5. Thermal conductivity as a function of temperature for the dyes.

The Seebeck coefficient is the defining characteristic of thermoelectric transport in materials. It is correlated to the point that the electrons carry both heat and charge. The electron density distribution in the material is determined by the temperature gradient, resulting in the opposite electric field and, hence, voltage, known as Seebeck voltage. The sign of the Seebeck coefficient spectrum and electrical conductivity is determined by the Seebeck voltage. This voltage is connected with an anti-symmetric distribution of electrons around the Fermi level. The Seebeck coefficient's high value is due to the anti-symmetry energy distribution of electrons passing through the material, which is linked to Fermi energy [20]. Figure 6 shows the Seebeck coefficient for dyes as a function of temperature. The following is an interpretation of the graph's behavior. Values at low temperatures are close to zero. The Seebeck coefficient is extremely low or negative, indicating that the thermal mobility of electrons is weak at first. Values climb with increasing temperature: As the temperature approaches 100 K, the Seebeck coefficient rises dramatically, reaching a peak value. This shows an increase in the voltage differential caused by heat transfer across the material. This action is prevalent in semiconducting materials, where a rise in thermal energy causes electrons or holes to move, hence amplifying the Seebeck effect. After peaking, the Seebeck coefficient steadily falls as the temperature rises more. This could be due to thermal scattering or exceeding the equilibrium point of positive and negative charge carriers.

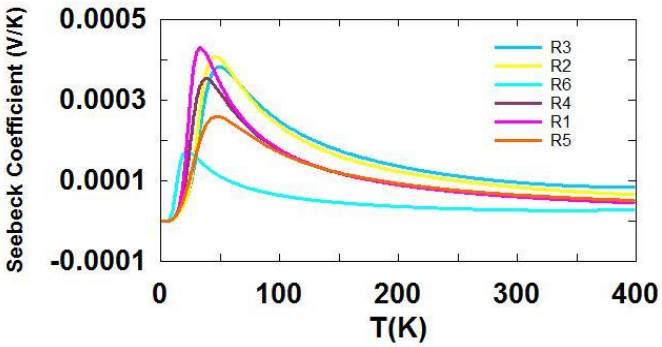

Figure 6. Seebeck coefficient as a function of temperature for the dyes.

4. Conclusions

Dye R6 had the highest electrical conductivity at the Fermi level (1.2×10^{-8} S) and relative conductance G/G_o (0.00305), showing that terminal functional groups play a substantial role in electronic performance. The study's findings revealed that electrical conductance gradually increases as temperature rises up to 180 K before stabilizing. Dye R2 displayed remarkable conductivity stability over the 180-400 K temperature range.The Seebeck coefficient increased significantly with temperature until it reached a peak, after which it began to progressively fall. This shows charge transport in the presence of a thermal gradient, which is typical for semiconducting materials. Dyes with less valuable symmetry performed better, which is consistent with earlier research indicating that reduced symmetry enhances molecule packing and stacking, boosting the efficiency of electronic transmission.

References

1. Melby, L. R.; Harder, R. J.; Hertler, W. R.; Mahler, W.; Benson, R. E.; Mochel, W. E. Substituted quinodimethanes. II. Anion-radical derivatives and complexes of 7,7,8,8-tetracyanoquinodimethane. J. Am. Chem. Soc.1962, 84, 3374–3387.10.1021/ja00876a029Search in Google Scholar
2. Zhou, Q., Song, K., Zhang, G. et al. Tetrathiafulvalenes as anchors for building highly conductive and mechanically tunable molecular junctions. Nat Commun 13, 1803 (2022). https://doi.org/10.1038/s41467-022-29483-2
3. Fang C, Li Y, Wang S, Liang M, Yan C, Liu J and Hong W (2025) Thermoelectric and thermal properties of molecular junctions: mechanisms, characterization methods and applications. Chemical Communications 61(23): 4447-4464.
4. Alves, H.; Molinari, A. S.; Xie, H.; Morpurgo, A. F. Metallic conduction at organic charge-transfer interfaces. Nat. Mater.2008, 7, 574–580.10.1038/nmat2205Search in Google ScholarPubMed
5. Bader, M. M.; Pham, P.-T. T.; Nassar, B. R.; Lin, H.; Xia, Y.; Frisbie, C. D. Extended 7,7,8,8-tetracyano-p-quinodimethane-based acceptors: how molecular shape and packing impact electron accepting behavior. Cryst. Growth Des.2009, 9, 4599–4601.10.1021/cg900939cSearch in Google Scholar
6. Tsubata, Y.; Suzuki, T.; Yamashita, Y.; Mukai, T.; Miyashi, T. Tetracyanoquinodimethanes fused with 1,2,5-thiadiazole and pyrazine units. Heterocycles1992, 33, 337–348.10.3987/COM-91-S44Search in Google Scholar
7. Suzuki, T.; Miyanari, S.; Kawai, H.; Fujiwara, K.; Fukushima, T.; Miyashi, T.; Yamashita, Y. Pyrazino-tetracyanonaphthoquinodimethanes: sterically deformed electron acceptors affording zwitterionic radicals. Tetrahedron2004, 60, 1997–2003.10.1016/j.tet.2004.01.005Search in Google Scholar
8. Ye, Q.; Chi, C. Recent highlights and perspectives on acene based molecules and materials. Chem. Mater.2014, 26, 4046–4056.10.1021/cm501536pSearch in Google Scholar
9. Ye, Q.; Chang, J.; Huang, K.-W.; Dai, G.; Chi, C. TCNQ-embedded heptacene and nonacene: synthesis, characterization and physical properties. Org. Biomol. Chem.2013, 11, 6285–6291.10.1039/c3ob40796aSearch in Google ScholarPubMed
10. Ye, Q.; Chang, J.; Huang, K.-W.; Dai, G.; Zhang, J.; Chen, Z.-K.; Wu, J.; Chi, C. Incorporating TCNQ into thiophene-fused heptacene for n-channel field effect transistor. Org. Lett.2012, 14, 2786–2789.10.1021/ol301014dSearch in Google ScholarPubMed
11. Brown, A. R.; de Leeuw, D. M.; Lous, E. J.; Havinga, E. E. Organic n-type field-effect transistor. Synth. Met.1994, 66, 257–261.10.1016/0379-6779(94)90075-2Search in Google Scholar
12. Handa, S.; Miyazaki, E.; Takimiya, K.; Kunugi, Y. Solution-processible n-channel organic field-effect transistors based on dicyanomethylene-substituted tetrathienoquinoid derivative. J. Am. Chem. Soc.2007, 129, 11684–11685.10.1021/ja074607sSearch in Google Scholar
13. Martin, N.; Segura, J. L.; Seoane, C.; Cruz, P. D. l.; Langa, F.; Orti, E.; Viruela, P. M.; Viruela, R. Synthesis and characterization of 11,11,12,12-tetracyano-1,4-anthraquinodimethanes (1,4-TCAQs): novel electron acceptors with photoinduced charge-transfer properties. J. Org. Chem.1995, 60, 4077–4084.10.1021/jo00118a025Search in Google Scholar
14. Yi, H. T.; Chen, Z.; Facchetti, A.; Podzorov, V. Solution-processed crystalline n-type organic transistors stable against electrical stress and photooxidation. Adv. Funct. Mater.2016, 26, 2365–2370.10.1002/adfm.201502423Search in Google Scholar
15. Xie, J.; Shi, K.; Cai, K.; Zhang, D.; Wang, J.-Y.; Pei, J.; Zhao, D. A NIR dye with high-performance n-type semiconducting properties. Chem. Sci.2016, 7, 499–504.10.1039/C5SC03045ESearch in Google Scholar
16. Zhang, C.; Zang, Y.; Gann, E.; McNeill, C. R.; Zhu, X.; Di, C-A.; Zhu, D. Two-dimensional π-expanded quinoidal terthiophenes terminated with dicyanomethylenes as n-type semiconductors for high-performance organic thin-film transistors. J. Am. Chem. Soc.2014, 136, 16176−16184.10.1021/ja510003ySearch in Google Scholar

17. Yan, H.; Chen, Z.; Zheng, Y.; Newman, C.; Quinn, J. R.; Dötz, F.; Kastler, M.; Facchetti, A. A high-mobility electron-transporting polymer for printed transistors. Nature2009, 457, 679−686.10.1038/nature07727Search in Google Scholar
18. J. E. M. Soler, E. Artacho, J. D. Gale, A. Garc´ıa, J. Junquera, P. Ordej´on, and D. S´anchez-Portal. “The SIESTA method for ab initio order-N materials simulation.”. Journal of Physics: Condensed Matter, 14: 2745–2779, 2002. DOI: https://doi.org/10.1088/0953- 8984/14/11/302.
19. E. Artacho, E. Anglada, O. Dieguez, J. D. Gale, A. Garcia, J. Junquera, R. M. Martin, P. Ordej´on, J. M. Pruneda, D. Sanchez-Portal, and J. M. Soler. “The SIESTA method; Developments and applicability.”. Journal of Physics: Condensed Matter, 20: 064208, 2008. DOI: https://doi.org/10.1088/0953- 8984/20/6/064208.
20. Oday A. Al-Owaedi, Hussein Neama Najeeb, Ahmed Kareem Obaid Aldulaimib, Nathera Hussin Alwan, Mohammed Shnain Alibd, Majed. Dwechb and Muneer A. AL-Da’amy " Thermoelectric Signature of d-orbitals in Tripod-Based Molecular Junctions" Materials Advances, Volume 5, Issue 24, 14 November 2024, Pages 9781-9791 doi.org/10.1039/d4ma00646a